Materials Science-Poland, *Vol. 27*, *No. 1*, *2009*

Preparation and bioactivity of embedded-style hydroxyapatite–titania nanotube arrays

X.-F. XIAO*, R.-F. LIU, T. TIAN

College of Chemistry and Materials Science, Fujian Normal University, Fuzhou 350007, China

Embedded-style hydroxyapatite–titania nanotube arrays were successfully prepared by anodic oxidation of titanium substrate and centrifugal filling hydroxyapatite precursor sol into hollow nanotubes. The morphology, microstructure and thermal stability of the samples were characterized by X-ray diffraction, environmental scanning electron microscopy, and energy dispersive X-ray analysis. The results show that the structure of titania nanotube arrays is stable at 500 °C or below, and the crystallized hydroxyapatite could be formed from hydroxyapatite precursor sol after calcining at 500 °C for 4 h. The optimum calcining temperature for this material is 500 °C. An obvious apatite layer formed on the surface of the embedded-style material after soaking in simulated body fluid for 5 days, indicating that the material possesses a good *in vitro* apatite forming ability on its surface.

Key words: *hydroxyapatite; bioactivity; composite; biomaterial; nanotube array; titania*

1. Introduction

Hydroxyapatite (HA, $Ca_{10}(PO_4)_6(OH)_2$), a major inorganic component of bones, shows high biocompatibility, bioactive and osteoconductive properties. HA, however, cannot be used in load bearing situations due to its brittleness [1, 2]. Titanium and its alloys possess favourable properties, such as good ductility, tensile and fatigue strength, modulus of elasticity matching that of bones, a similar density to that of bones, and good biocompatibility. So they are frequently used as surgical implants in load bearing situations such as hip prostheses and dental implants [3, 4]. However, it is difficult for them to bond to bones, due to their poor osteointegration properties. Thus, much attention has been focused on improving the bioactivity of titanium, using techniques such as plasma spray [5], laser fusion [6], ion sputtering [7], electrophoretic deposition [8], hydrothermal electrodeposition [9] etc. to form HA coating on titanium substrates. All these methods have respective merits but they share a common ground in that the materials derived from them are layer-style configurations, with HA

*Corresponding author, e-mail: rfliu@vip.sina.com

coating on the surface of titanium substrates. This means that the interfacial fractures may occur between HA coatings and titanium substrates, resulting in the implant migration and loss. Therefore, how to avoid loosing and scaling-off of coating is an urgent problem to resolve for HA coating materials.

In this study, a new embedded-style composite material, instead of a layer-style one, was prepared by anodizing on the titanium in HF solution to fabricate titania nanotube arrays and then affusing HA precursor sol into titania nanotubes by centrifugal force. HA precursor sol was prepared from $Ca(NO_3)_2 \cdot 4H_2O$ ethanol solution and P_2O_5 ethanol solution. Titania nanotube arrays prepared by anodic oxidation in HF [10–14] show a discrete, well-ordered, and hollow structure. Therefore, titania nanotube arrays could be used as carriers to fill HA precursor sol. Consequently, an embedded-style hydroxyapatite–titania nanotube arrays composite material could be obtained. This composite material has both excellent properties of HA and Ti being expected to improve the loosing and dislocation problems of HA coating.

2. Experimental

Preparation of titania nanotube arrays. Pure titanium foils (99.5% pure) were purchased from the Northwest Institute for Non-ferrous Metal Research (China). Prior to anodization, the titanium foils were ultrasonically cleaned in acetone and distilled water, for 5 min, respectively, then eroded in 4% HF + 5mol/dm^3 HNO_3 for 30 s, followed by ultrasonic cleaning in distilled water for 5 min and dried in air at 40 °C. A set-up with a graphite cathode was employed for the anodization of titanium in HF solution (0.5 wt. %). All electrolytes were prepared from analytical reagent grade chemicals and distilled water. The anodizing voltage was kept constant at 20 V during the entire process with a dc power supply (GOA, China) [10]. The whole course of anodization was conducted at room temperature (25 °C) with magnetic agitation. After anodization, the samples were rinsed with distilled water and then dried at 40 °C in air. The effect of the heat treatment on morphology of the titania nanotube arrays was conducted by putting the samples into a furnace at various temperatures (from 300 °C to 600 °C) for 4 h.

Preparation of the HA precursor sol. HA precursor sol was prepared using a mixed ethanol solution of calcium nitrate and phosphorous pentoxide [15], controlling the Ca/P molar ratio at 1.67 being the stoichiometric value of HA. Calcium nitrate ethanol solution was dripped into phosphorous pentoxide ethanol solution with a magnetic agitation at room temperature, and kept static for 24 h before filling into titania nanotube arrays. Furthermore, another precursor sol was dried at 100 °C for 2 h and the resulting dried gels were calcined for 4 h at various temperatures, ranging between 300 °C and 500 °C.

Preparation of embedded-style composite materials. The prepared HA precursor sol was placed in a centrifugal test-tube, and then the prepared titania nanotube arrays

were soaked in the HA precursor sol. The samples were placed as shown in Fig. 1, titanium foil was glued horizontally on the built-in sample stage and titania nanotube arrays were put upwards. Under the centrifugal force, produced by the centrifuge operating at 4000 rev./min for 30 min, HA precursor sol was filled into the titania nanotubes. The samples were then taken out, ultrasonically cleaned in pure ethanol to remove HA precursor sol on the top of titania nanotube arrays. Then, the samples were dried at 100 °C in air for 1 h and calcined at 500 °C for 4 h.

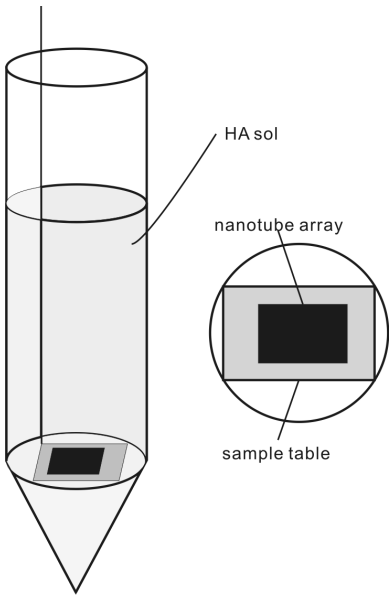

Fig. 1. Schematic diagram of the placement of the sample during centrifugal filling

In vitro bioactivity of the composite material. The composite materials were inserted into culture vials containing a simulated body fluid (SBF), which was prepared according to Kokubo et al. [16]. The composite materials were soaked in SBF for 5 days at 37 °C without stirring before they were taken out for coating characterization. Titania nanotube arrays without embedded HA were also soaked in SBF in a control experiment.

Characterization of the samples. A Philips XL30 environmental scanning electron microscope (ESEM), equipped with a Philips energy dispersive X-ray analyzer (EDAX) was employed to characterize the morphology and compositions of the composite materials. In order to obtain information on the structure of composite materials, they were mechanically bent, and in some cases a partial lift-off of the titanium substrate occurred. A Philips X'Pert MPD diffractometer system, using CuK_α radiation, was employed to characterize the phase of the samples. The X-ray generator operated at 40 kV and 40 mA. Data sets were collected over the range of 5–90° with a step size of 0.02° and a count rate of 4.0 $K \cdot min^{-1}$.

3. Results and discussion

Figure 2 shows SEM images of the titania nanotube arrays obtained by anodization. As shown in Fig. 2a, titania nanotube arrays with discrete, hollow, tubular features were obtained in 0.5 % HF solution. The SEM micrographs show that titania nanotubes measure about 250 nm long with an inner diameter of about 100 nm. This structure possesses larger surface areas and is different from the nonporous titania layers formed in other electrolytes such as sulfuric acid [17, 18]. In fluoride-containing electrolytes, anodization of titanium is accompanied with the chemical dissolution of titanium oxide due to the formation of TiF_6^{2-}. Highly uniform nanotube arrays, instead of porous or nonporous structures, formed [10, 14]. Although the shrinkage of the tube diameter was observed after heating at 500 °C for 4 h (Fig. 2b), the structure of the titania nanotube arrays is still intact. When increasing the heat treatment temperature to 600 °C (Fig. 2c), the nanotubes collapse into an irregularly shaped morphology, losing their tubular structures. The results indicate that the titania nanotube arrays structure could be stable at temperatures not higher than 500 °C.

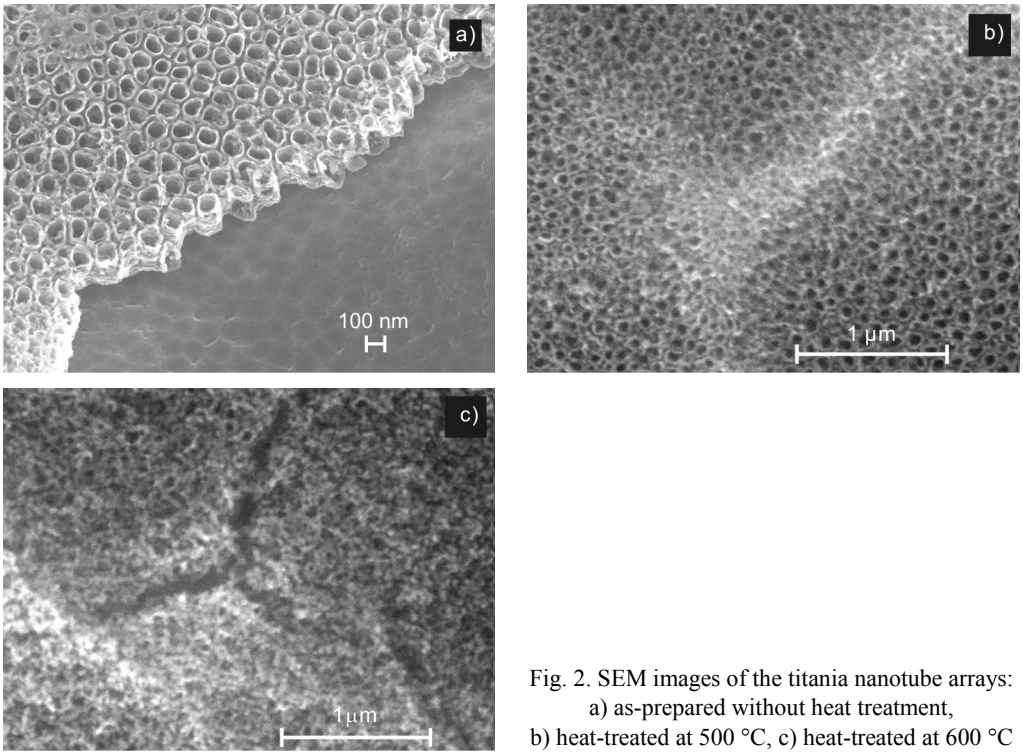

Fig. 2. SEM images of the titania nanotube arrays: a) as-prepared without heat treatment, b) heat-treated at 500 °C, c) heat-treated at 600 °C

Figure 3 shows the XRD patterns of the titania nanotube arrays without (Fig. 3a) or with heat treatment at 500 °C (Fig. 3b). Only Ti diffraction peaks can be seen in Fig. 3a, indicating that the untreated nanotubes were amorphous and were crystallized

from amorphous to anatase phase at 500 °C. In order to testify the crystallization of titania nanotube arrays, the same heat treatment was performed on pure titanium without titania nanotube arrays. There is only Ti peak appearing on the pattern at 500 °C. The results indicate that the phase transformation of the titania nanotube arrays at 500 °C is the result of their crystallization.

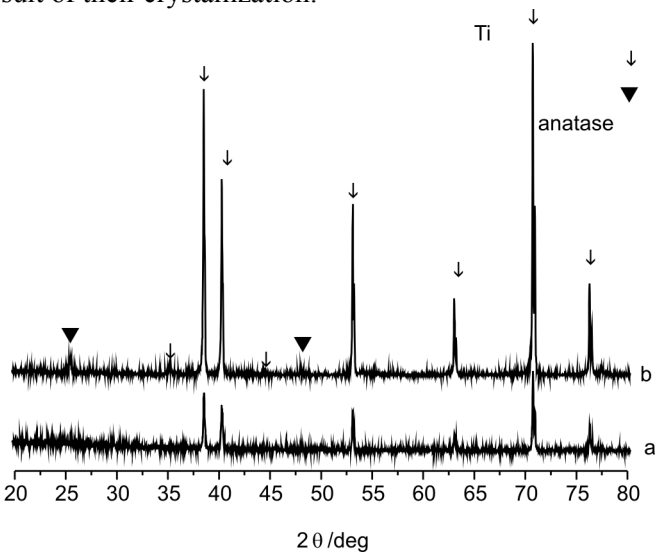

Fig. 3. XRD patterns of titania nanotube arrays: a) as-prepared without heat treatment, b) heat-treated at 500 °C

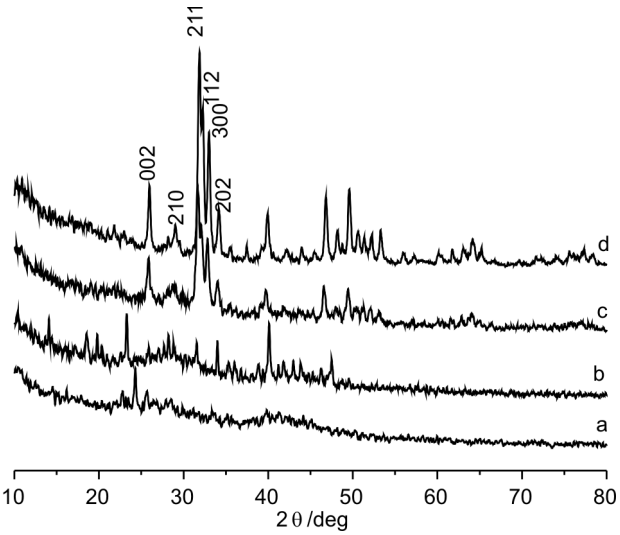

Fig. 4. XRD patterns of the powder from HA precursor sol after calcining at various temperatures: a) before calcining, b) at 300 °C, c) at 400 °C, d) at 500 °C

Figure 4 shows the XRD patterns of the powder formed from HA precursor sol after calcining at various temperatures. Figure 4a shows that the dried gel without heat treatment exhibits highly amorphous characteristics. The powder calcined at 300 °C exhibits many diffraction peaks of other phases with a considerable amount of amorphous phase (Fig. 4b). The diffraction peaks of apatite appear after heat treatment at 400 °C (Fig. 4c), and their intensity increases with increasing temperature. After calcining at 500 °C, the intensity of the main diffraction peaks of HA, such as (002), (210), (211), (112), (300) and (202), is very strong, indicating that HA has a high degree of crystallinity.

According to the morphology observation of titania nanotube arrays (Fig.2) and the XRD analysis of the powder of HA dried gel after heat treatment at different temperature (Fig. 4), an embedded-style hydroxyapatite–titania nanotube arrays composite material could be obtained by affusing HA precursor sol into titania nanotubes using centrifugal force and then calcining at 500 °C. The optimum calcining temperature for this material is 500 °C.

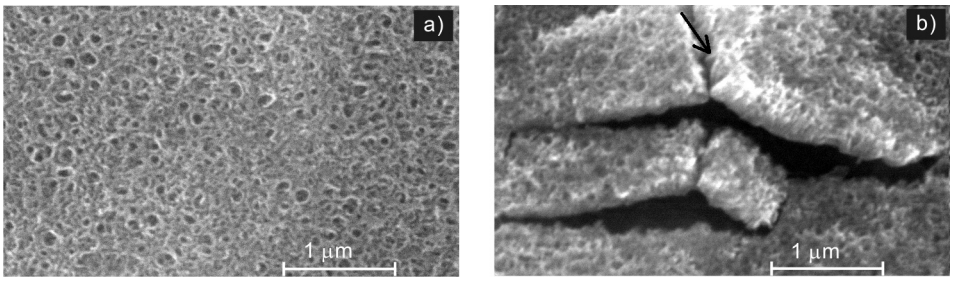

Fig. 5. SEM image of the surface and transection morphology of the embedded-style materials

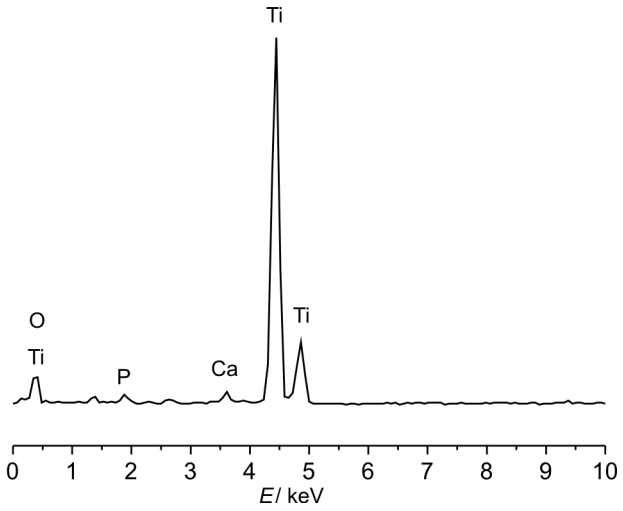

Fig. 6. EDAX analysis of the nanotube end as shown with the arrow in Fig. 5b

Figure 5 shows the surface and transection morphology of the embedded-style hydroxyapatite–titania nanotube arrays composite material. As shown in Fig. 5a, it is clear that many tubes have been filled with something, but some nanotubes still have not been filled with, the mouths of which are clearly visible. In order to confirm whether the HA precursor sol has been filled into the nanotubes, the nanotube end was characterized by EDAX, as shown in the arrow in Fig.5b. EDAX results show that titania nanotube arrays mainly consist of Ti, O and a small quantity of Ca and P element (Fig.6), which indicates that HA precursor sol could be filled into the nanotube using centrifugal force, and such embedded-style hydroxyapatite–titania nanotube arrays composite material could be obtained.

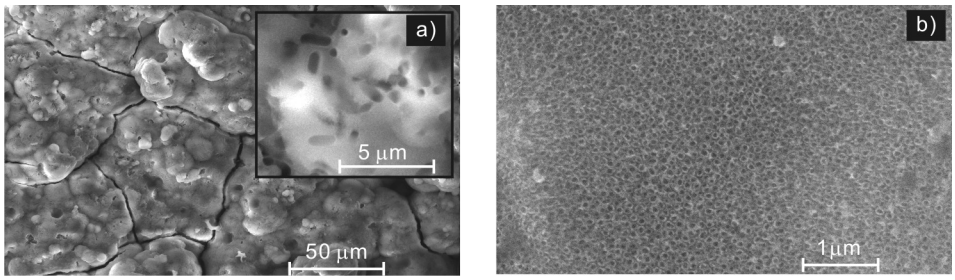

Fig. 7. Surface morphology of the sample after soaking in SBF for 5 days:
a) embedded-style composite material, b) titania nanotube arrays heat-treated at 500 °C

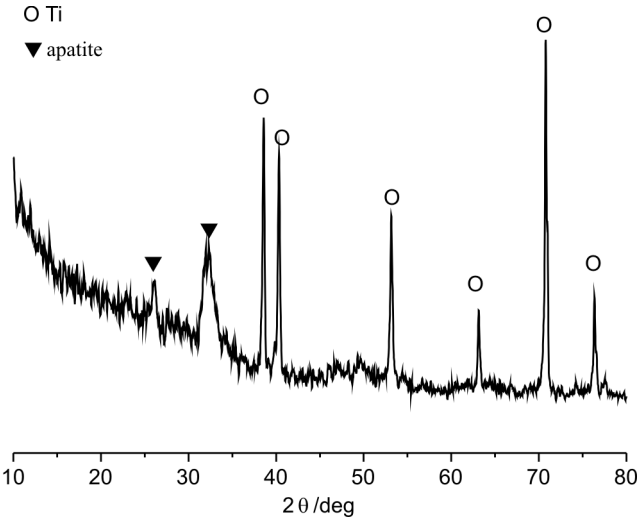

Fig. 8 XRD pattern of the new layer after soaking in SBF for 5 days

Figure 7a shows the surface morphology of the embedded-style hydroxyapatite –titania nanotube arrays after soaking in SBF for 5 days with an obvious layer formed on the surface of the titania nanotube arrays. The XRD pattern of the new layer is shown in Fig. 8, compared with the standard card (JCPDS 09-432), indicating

that the layer formed on the surface is an apatite layer. The results of a control experiment without filling HA precursor sol are shown in Fig. 7b: there is nothing on the surface of the titania nanotube arrays and the open tops of the nanotubes are clearly visible. The results show that an embedded-style hydroxyapatite–titania nanotube arrays composite material has an apatite-forming ability in SBF on its surface related to the HA contained in the nanotubes. After soaking in SBF, a trace of HA could dissolve and form PO_4^{3-} and Ca^{2+} ions which induce the nucleation of apatite. Once the apatite nuclei are formed, they spontaneously grow by consuming calcium and phosphate ions from SBF. As a result, apatite nucleates and grows on the surface of titania nanotube arrays. Therefore, they are endowed with *in vitro* bioactivity by centrifugal filling with the HA sol.

4. Conclusions

A new embedded-style hydroxyapatite–titania nanotube arrays composite material was successfully prepared by centrifugal filling HA precursor sol into the nanotubes of titania nanotube arrays, with the aid of the pressure provided by a centrifuge. The optimum calcining temperature for this embedded-style material is 500 °C. Bioactivity study indicates the obtained material possesses excellent bioactivity. It is an effective way to endow Ti with bioactivity by anodic oxidation in HF electrolyte and centrifugal filling HA precursor sol into the nanotubes.

Acknowledgements

The authors thank the National Nature Science Foundation of China (30600149), the Science Research Foundation of the Ministry of Health and United Fujian Provincial Health and Education Project for Tackling the Key Research, PR China (WKJ 2005-2-008), Fujian Development and Reform Commission of China (No. 2004 (477)), Fujian Provincial Department of Science and Technology (No. 2006I0015) and Fujian Nature Science Foundation (2007J0144).

References

[1] OSBORN J., NEWESELY H., Biomater., 1 (1980), 108.
[2] AKAO H., AOKI H., KATO K., J. Mater. Sci., 16 (1981), 809.
[3] NOORT R., J. Mater. Sci., 22 (1987), 3801.
[4] TENGVALL P., LUNDSTROM I., Clin. Mater., 9 (1992), 115.
[5] SUN L., BERNDT C.C., KHOR K.A., CHEANG H.N., GROSS K.A., J. Biomed. Mater. Res., 2 (2002), 228.
[6] PILLIAR R.M., FILIAGGI M.J., Bioceramics 6 (1993), 165.
[7] ONG J.L., LUCAS L.C., Biomater., 14 (1994), 337.
[8] DUCHEYNE P., RADIN S., HEUGHEBAERT M., HEUGHEBAERT J.C., Biomater., 11 (1990), 244.
[9] XIAO X.F., LIU R.F., ZHENG Y.Z., Mater. Lett., 59 (2005), 1660.
[10] GONG D.W., GRIMES C.A., VARGHESE O.K., HU W., SINGH R.S., CHEN Z., DICKEY E.C., J. Mater. Res., 12 (2001), 3331.
[11] BERANEK R., HILDEBRAND H., SCHMUKI P., Electrochem. Solid-State Lett., 3 (2003) B12.
[12] MOR G.K., SHANKAR K., PAULOSE M., VARGHESE O.K., GRIMES C.A., Nano Lett., 1 (2005), 191.

[13] CAI Q., PAULOSE M., VARGHESE O.K., GRIMES C.A., J. Mater. Res,. 1 (2005), 230.
[14] MOR G.K., VARGHESE O.K, PAULOSE M., MUKHERJEE N., GRIMES C.A., J. Mater. Res., 11 (2003), 2588.
[15] WENG W.J., BAPTISTA J.L., J. Mater. Sci.: Mater. Med., 9 (1998), 159.
[16] KOKUBO T., KUSHITANI H., SAKKA S., KITSUGI T., YAMAMURO T., J. Biomed. Mater. Res., 24 (1990), 721.
[17] YANG B.C., UCHIDA M., KIM H.M., ZHANG X.D., KOKUBO T., Biomater., 25 (2004), 1003.
[18] SUL Y.T., JOHANSSON C.B., JEONG Y., ALBREKTSSON T., Med. Eng. Phys., 23 (2001), 329.

Received 3 September 2007
Revised 22 August 2008